Temperature variability over Dokriani glacier region, Western Himalaya, India

Article *in* Quaternary International · June 2023

DOI: 10.1016/j.quaint.2023.05.013

6 authors, including:

Jayendra Singh
Wadia Institute of Himalayan Geology
38 PUBLICATIONS **1,409** CITATIONS
SEE PROFILE

Nilendu Singh
Wadia Institute of Himalayan Geology
54 PUBLICATIONS **290** CITATIONS
SEE PROFILE

Dr. Pankaj Chauhan
Wadia Institute of Himalayan Geology
39 PUBLICATIONS **132** CITATIONS
SEE PROFILE

Ram Yadav
Birbal Sahni Institute of Palaeobotany
64 PUBLICATIONS **2,333** CITATIONS
SEE PROFILE

Quaternary International 664 (2023) 33–41

Contents lists available at ScienceDirect

Quaternary International

journal homepage: www.elsevier.com/locate/quaint

Temperature variability over Dokriani glacier region, Western Himalaya, India

Tanupriya Rastogi [a], Jayendra Singh [a,*], Nilendu Singh [a], Pankaj Chauhan [a], Ram R. Yadav [a], Bindhyachal Pandey [b]

[a] Wadia Institute of Himalayan Geology, Dehradun, 248001, India
[b] Department of Geology, Banaras Hindu University, Varanasi, 221 005, India

ARTICLE INFO

Keywords:
Climate reconstruction
March–June temperature
Tree-ring
Dokriani glacier
Western Himalaya
India

ABSTRACT

Long-term climate records which help decipher past climate variability and its impact are scarce in the tough terrain of the Himalayan region. Therefore, in order to fill the climate data gap and understand the glacier climate linkage, we developed a 231 year long (1785–2015 CE) March–June temperature record using ring-width chronology of Himalayan fir (*Abies pindrow* (Royle ex D.Don) Royle) for the Din Gad valley, Dokriani glacier region, Uttarkashi, Uttarakhand, in the Western Himalaya. The Din Gad, originating from the Dokriani glacier, is a meltwater river contributing to Bhagirathi catchment in the headwaters of the socio-economically vital Ganga River. The 21-year running mean of the temperature record showed 1978–1998 CE as the coldest period followed by 1925–1945 CE, and 1890–1910 CE as the warmest period followed by 1946–1966 CE over the entire time series. The reconstruction matches well with tree-ring based temperature records available from the Garhwal Himalaya. It also shows similarity to tree-ring based temperature reconstructions from the Western Himalaya, Nepal, Tibetan Plateau and Bhutan, thus displaying a regional scale climate signal. The low frequency fluctuation patterns of the March–June temperature also matches with Asia and Northern hemisphere temperature records. Reconstructed March–June temperature record showed a statistically negligible warming temperature trend during 1901–1989 CE in the 20th century. It, however, captured a warming spike from 1990s CE which continues rising into the 21st century, which is also evident in the Northern hemisphere temperature record. Moreover, temperature rise is not anomalous in the past 231 years and well within range of the rest of the series. The present temperature record exclusively from the glacier region revealed a strong linkage with the benchmark Dokriani glacier's winter mass balance (November–April) revealing mass loss (gain) episodes occurred in warm (cool) phases. This first such record from the glacier valleys in Ganga headwaters would be of great value at providing insight into past climate variability and glacier behaviour with respect to climate change in long term perspective, and thus would provide valuable information for water resource management in light of climate change.

1. Introduction

Inter-hemispheric temperature records coherently reflect an unprecedented warm phase in the latter half of the 20th century relative to the past millennium, testifying the signal of recent warming at a global scale (Neukom et al., 2014). Global surface temperature rise of 1.09 °C over 2011–2020 CE in comparison to 1850–1900 CE is unprecedented in the past 2000 years (IPCC, 2021). Recent warming is linked with the rise in extreme precipitation and heat events and is also projected to cause a persistent rise in their magnitude and frequency overtime (Meehl and Tebaldi, 2004; Fischer and Knutti, 2015; Horton et al., 2016). The temperature rise is affecting the global climate (Dai, 2013; Donat et al., 2016) and, consequently, the biosphere (Teskey et al., 2015; Worm and Lotze, 2021), including the human systems (Levy and Patz, 2015; Duchenne-Moutien and Neetoo, 2021).

High altitude areas of the world are particularly vulnerable to the warming climate. The rate of temperature rise in these regions is more acute with increasing altitude and shows much higher variability (Diaz and Bradley, 1997; Ohmura, 2012; Pepin et al., 2015). This is apparent most significantly in the Himalayan region (Ohmura, 2012) where

* Corresponding author.
E-mail address: jayendrasingh@wihg.res.in (J. Singh).

https://doi.org/10.1016/j.quaint.2023.05.013
Received 20 September 2022; Received in revised form 16 May 2023; Accepted 22 May 2023
Available online 1 June 2023

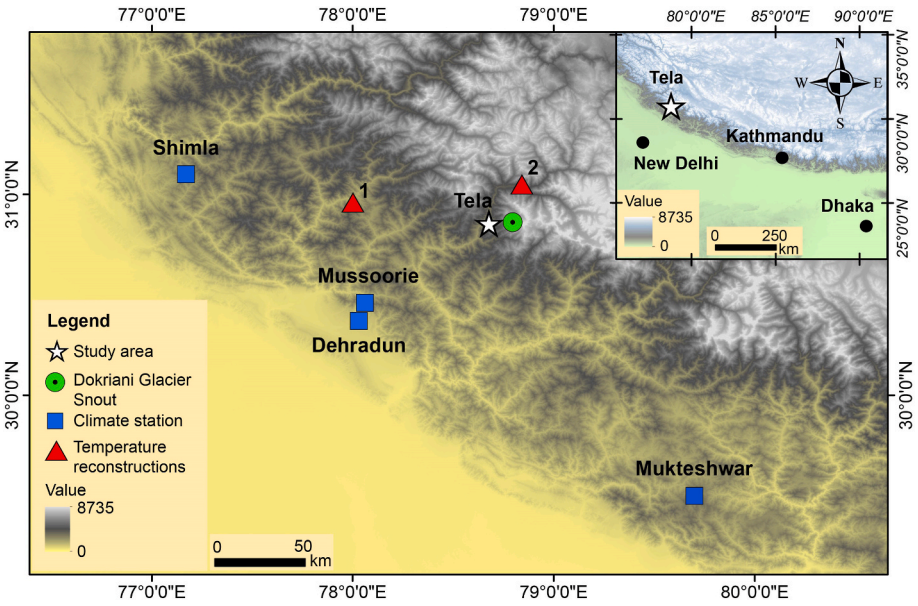

Fig. 1. Map showing location of tree-ring study area, meteorological station used in the present study and tree-ring based temperature reconstructions (1-Singh and Yadav, 2014 and 2-Yadav et al., 2004) used in comparison.

maximum warming has been observed at higher altitudes (Shrestha et al., 1999). The temperature here has been warming at a rate three times higher than global average (Xu et al., 2009). In the Western Himalaya, the annual temperature has warmed by 1.6 °C in the 20th century, however higher temperatures were observed in winters relative to other seasons (Bhutiyani et al., 2007; Mondal et al., 2015; Sonali et al., 2017). An abrupt rise in annual temperature trend has also been noticed from 1990s. (Bhutiyani et al., 2007). With projected warming, the High Mountains of Asia are estimated to lose 36 ± 7% ice mass from its glaciers by the end of the 21st century, even if we succeed in curbing global temperature rise to 1.5 °C, as per the Paris Agreement of 2015 (Kraaijenbrink et al., 2017). The long-term net mass balance for glaciers in the Indian Himalaya also reveal mass loss for the past four decades with a few exceptions (Pratap et al., 2016). This region is home to large river systems that emerge from these vast ice sanctuaries and supports among the highest population densities on the planet, along with being home to biodiversity hotspots. Given this scenario and the anticipated socioeconomic and ecological impact of warming, it is essential to investigate the long-term climate variability and its impact on glacier behaviour in order to devise effective adaptation and mitigation strategies for the adversity caused by glacier decay. The paucity of long-term instrumental climate data in Himalayan terrain has been addressed to a certain extent by tree-ring based climate reconstructions from the Eastern (Bhattacharyya and Chaudhary, 2003; Krusic et al., 2015), Central (Sano et al., 2005; Thapa et al., 2015; Aryal et al., 2020) and Western Himalaya (Singh and Yadav, 2014; Yadav et al., 1997, 1999), along with the Tibetan plateau region (Zhu et al., 2011). But, tree ring based temperature reconstructions from close vicinity of glaciers are few and, particularly, from the Western Himalaya are limited, with only one such temperature record (August–September) from the Uttarkashi district of Uttarakhand (Chaudhary et al., 2013).

The Dokriani glacier, located in proximity of Bhagirathi river catchment in Uttarkashi, is among the best studied glaciers in the Indian Himalaya considering the multifarious studies on its mass balance (Dobhal et al., 2008; Pratap et al., 2016; Azam and Srivastava, 2020), recession (Dobhal et al., 2004; Dobhal and Mehta, 2010), hydrological (Hasnain and Thayyen, 1999; Hasnain et al., 2001; Singh et al., 2004; Thayyen et al., 2007; Thayyen and Gergan, 2010; Pratap et al., 2015) and meteorological aspects (Thayyen et al., 2005; Kumar et al., 2014). But in spite of these, no long-term climate record exists for this area which could greatly expand the scope of studies on this glacier with regard to its dynamics in the long-term perspective. This becomes essential as the Dokriani glacier along with the Gangotri glacier forms part of the system of glaciers that contribute to the Bhagirathi River system that eventually merges with the Alaknanda River to form the socioeconomically and culturally vital, river Ganga. Recognising the importance of climate variability in this region and to address this gap, we prepared a ring-width chronology of *Abies pindrow (A. pindrow)* from the Din Gad valley with the aim to develop a temperature record for the Dokriani glacier region and explore its potential in unveiling glacier behavior in long-term perspective.

2. Regional setting

The study site, Tela, lies in the Din Gad valley in the Uttarkashi district, Uttarakhand (Fig. 1), and is a part of the Bhagirathi catchment that forms the headwaters of the river Ganga. Tela is situated on the left bank of river Din Gad which is a proglacial meltwater stream originating from the Dokriani glacier ~12 km away aerially. The Dokriani glacier (30°50′ N and 78°50′ E) is a valley type glacier that is formed by the merging of two cirques bound by the western slope of Jaonli peak (6632 m a.s.l.) and the northern slope of Draupadi ka Danda peak (5716 m a.s.l.) (Garg et al., 2022). The Dokriani glacier is ~5 km in length and has an area of 7.03 km^2 while the area of Dokriani glacier catchment is 15.71 km^2 (Azam and Srivastava, 2020). The glacier has a northwest orientation and is bound by two large lateral moraines.

Geologically the area is bound by two major thrusts – the Munsiari Thrust (MCT-1) in the south and the Trans Himadri Fault (THF) to the north (Heim and Gansser, 1939; Valdiya, 1998). The region comprises of metamorphic and granitic rocks. The climate is influenced by both the Indian Summer Monsoon (ISM) and the Westerlies. The ISM contributes ~71% of the annual precipitation during June to September whereas remaining occurs in the rest of the months (Singh et al., 2019).

3. Material and methods

3.1. Tree-ring data and chronology development

Himalayan fir (*A. pindrow* (Royle ex D.Don) Royle), a constituent of Mid-montane needle-leaf evergreen forest formation type (Champion

Table 1
March–June temperature reconstruction calibration-verification statistics obtained in linear regression analysis.

Calibration		Verification						
Period	ar^2%	Period	r	T value	Sign test	RE	CE	RMSE
1898–1956	42	1957–2015	0.655 ($p < 0.00001$)	3.68 ($p = 0.0005$)	$43^+/16^-$($p = 0.0006$)	0.416	0.415	0.725
1957–2015	42	1898–1956	0.655 ($p < 0.00001$)	5.14 ($p < 0.00001$)	$43^+/16^-$($p = 0.0006$)	0.420	0.419	0.794
1898–2015	42							

Note: ar^2 is captured variance adjusted for degrees of freedom which explains the percent variation in the dependent variable that can be explained by variation in the independent variable in a regression; r is Pearson correlation coefficient which gives strength of association between the independent and dependent variable; RE is the reduction of error and CE is coefficient of efficiency (Fritts, 1976). Both are used for verification purposes in reconstructions where positive values indicate the climatological potential (Cook et al., 1999). RMSE is root mean square error explains standard deviation of unexplained variance. The two tailed p values are given in brackets.

and Seth, 1968), was selected for the present study. It is found in the Western Himalaya in pure forest stands or as a part of *Picea-Cedrus-Abies pindrow-Pinus wallichiana* forest assemblage at elevations of 2500–3000 m a.s.l. or higher (Champion and Seth, 1968). The cores were sampled at Tela (2534 m a.s.l.), Uttarkashi, Uttarakhand, on the left bank of the Din Gad River, which emerges from the snout of Dokriani glacier approximately ~12 km away aerially, and is a tributary to the Bhagirathi river system (Fig. 1). *A. pindrow* trees were growing on an east facing slope in a mixed deciduous evergreen conifer forest stand comprising *Picea smithiana* (Wall.) Boiss and *Aesculus indica* (Wall. ex Camb.) (Singh et al., 2019) along with *Quercus, Carpinus, Pinus, Taxus, and Cedrus* which represent the forest assemblage at the altitude (Phadtare, 2000; Bhattacharyya et al., 2011). Cores were retrieved from trees that were old and undisturbed, and those with any visible marks of injury were avoided. Tree cores were extracted using an increment borer at 1.37 m above the ground and processed in the laboratory using standard dendrochronological techniques (Stokes and Smiley, 1968; Fritts, 1976). The annual growth rings of each core were measured using the LINTAB measuring system that measures up to 0.001 mm precision (Rinntech, Heidelberg, Germany) and each growth ring was then crossdated using the TSAP program (Rinn, 2003). The quality of dating and measurement was crosschecked in COFECHA software to filter out any dating and measurement errors (Holmes, 1983). Finally, 34 cores (21 trees) were used for further analysis. The individual ring-width series were standardized using the program ARSTAN to remove age-size related growth trends and disturbances due to stand dynamics (Cook et al., 1990). Out of total 34 cores, 26 cores were detrended with a smoothing spline of 2/3rd of the series length while 8 series were treated with a 50 year cubic spline to account for growth dynamics different than the rest of the series. Finally, a mean chronology was generated by applying biweight robust mean.

3.2. Climate data

The tough terrain and high elevation of the Himalaya make it logistically difficult to put in place and maintain a systematic, widespread meteorological observation network. For the present study, to understand ring-width chronology and climate relationship we used climate data of nearby available homogenous datasets from climate stations [Shimla (2202 m a.s.l.), Mussoorie (1988 m a.s.l.), Dehradun (682 m a.s.l.) and Mukteshwar (2311 m a.s.l.)]. We also used regional climate data series prepared using these four stations and gridded data of the sampling location to test the relationship (Fig. 1). The regional climate data series was prepared by converting individual station data of the four stations (Shimla, Mussoorie, Dehradun and Mukteshwar) to anomalies with respect to their mean and standard deviation over the common period, and then these anomalised series were averaged. The tree growth-climate analysis revealed weak relationship with temperature of Shimla, Dehradun and the regional climate series. Mukteshwar and Mussoorie temperature data showed significant correlation with the chronology while CRU gridded data showed a slightly weaker correlation. However, combining the Mussoorie and Mukteshwar climate data could not enhance the signal and therefore, we used Mukteshwar data available up to recent time (2311 m a.s.l.; 1897–2019 CE) in further analysis (http://climexp.knmi.nl/). This station best represents our study area in terms of its 1) climate regime and 2) flora at similar elevation (Shah and Joshi, 1971; Negi, 2000). The dataset has been used by multiple tree ring-based climate studies in the Western Himalaya region for precipitation (Singh and Yadav, 2005; Singh et al., 2006; Yadav and Park, 2000) and temperature reconstructions for Nepal (Sano et al., 2005; Thapa et al., 2013, 2015) and Garhwal region (Chaudhary et al., 2013). This further highlights the reliability and suitability of the Mukteshwar station record for climate analysis in the Western Himalaya. Finally, for developing the reconstruction we adjusted the temperature data of Mukteshwar station using the lapse rate estimated by Kattel et al. (2013), in order to account for the elevation difference between the study area and the climate station (Supplementary Fig. S1). Climate data show that maximum temperature in this region is recorded in June while the lowest is observed in January. The region receives most of the precipitation in the monsoon months (June–September) with highest rainfall in July and minimum in November (Supplementary Fig. S1).

3.3. Tree growth-climate relationship

For analyzing the relationship of tree growth with climate, correlation analyses was performed between standard ring-width chronology of *A. pindrow* and Mukteshwar precipitation and temperature data over a common period (1898–2015 CE). As cambial activity of *A. pindrow* starts in April/May and ceases in month of October, climate data of previous year October to October of the following year was taken in correlation analyses using program DENDROCLIM2002 (Biondi and Waikul, 2004). Although cambial activity stops in winter, the photosynthetic food reserves generated are utilized at the commencement of the ensuing year's growth (Malik et al., 2020). Signal identified in the climate analyses was further used to develop climate record.

3.4. Temperature reconstruction

We used linear regression analyses to develop the reconstruction. In order to validate the calibration models the temperature series was split into two sub-periods (1898–1956 CE and 1957–2015 CE) and each of these sub-periods were validated with their respective verification periods. Both the calibration models were rigorously verified using multiple statistical analyses [Reduction of error (RE), Pearson correlation coefficient, sign test, coefficient of efficiency (CE), Root mean square error (RMSE) and *t*-test (Fritts, 1976; Cook et al., 1999)] in their respective verification periods (Table 1). To capture low frequency signals the entire instrumental temperature series (1898–2015 CE) was used in developing the reconstruction.

To explore the potential association between the reconstructed temperature record and glacier fluctuations we used reconstructed mass balance data (1979–2018 CE) developed by Azam and Srivastava (2020). The mass balance time series was developed on the basis of a

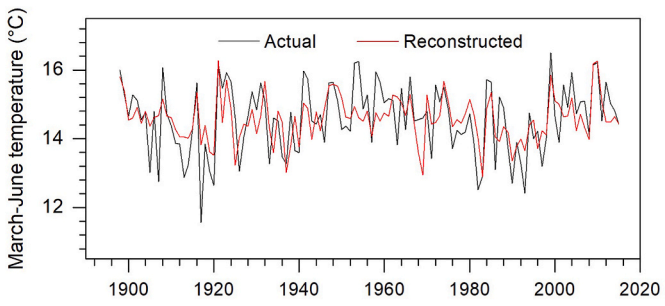

Fig. 2. Instrumental March–June temperature data (black line) plotted with corresponding months' reconstruction (red line) for the period (1898–2015 CE).

glacier mass balance model that comprised an accumulation module and temperature index ablation module made using the ERA5 daily temperature and precipitation data (1979–2018 CE) (Azam and Srivastava, 2020).

We also performed spatial correlation analysis between our temperature series and March–June CRU TS4.01 temperature data (1901–2015 CE) using KNMI climate explorer (http://climexp.knmi.nl/) to understand regional scale features in our data.

4. Results and discussion

4.1. Ring-width chronology

We developed a ring-width chronology spanning 360 years (1656–2015 CE) which was truncated at 1785 CE as Expressed Population Signal (EPS) (Wigley et al., 1984) was ≥0.85 (Supplementary Fig. S2). Mean sensitivity which is a measure of year to year variability in ring-width chronology was 0.161 and mean rbar, that is the mean correlation among ring-widths of all the trees, was 0.427. The standard deviation depicting the variability in the series was 0.171. High mean sensitivity, rbar and standard deviation point towards the dendroclimatic potential of the chronology.

4.2. Tree growth-climate response analysis

The present study registered a significant inverse relationship between temperature and radial growth in *A. pindrow* extending from previous years' October to ensuing year June, and August, while precipitation had a significant direct relationship with growth in January, March and April (Supplementary Fig. S3). This signifies that sufficient moisture availability with low temperatures is ideal for growth of *A. pindrow* in the Din Gad valley in these months. (Supplementary Fig. S3). Whereas rise in temperature in premonsoon months (March-April-May) combined with low precipitation causes moisture deficiency in soil. This causes plant stress and increases evapotranspiration resulting in reduced cambial activity at high elevation regions under the influence of strong solar radiation (Borgaonkar et al., 1996, 1999). This results in a negative relationship between tree growth and temperature during March–May. However, slightly more than average precipitation in these months causes replenishment of minimum moisture levels and positively aids growth (Borgaonkar et al., 1996). A similar negative response of *A. pindrow* to premonsoon temperature was also observed in other studies from the Western (Borgaonkar et al., 1999; Ram, 2012) and Central Himalayan region (Thapa et al., 2013). We also performed correlation analysis of chronology with the Palmer Drought Severity Index (PDSI) which revealed a poor relationship that was found unsuitable for reconstruction. And finally, the significant strong relationship with March–June temperature was used in developing temperature reconstruction for the region.

Table 2
A 5-year, 11-year and 21-year running means of March–June temperature reconstruction.

Period	Cool (°C)	Period	Warm (°C)
5 Year			
1788–1792	13.35	1890–1894	15.43
1989–1993	13.79	1802–1806	15.37
1851–1855	13.93	1946–1950	15.34
1934–1938	13.95	2009–2013	15.29
1835–1839	13.98	1846–1850	15.18
11 Year			
1986–1996	13.99	1890–1900	15.22
1786–1796	14.14	1946–1956	14.98
1910–1920	14.18	2000–2010	14.93
1933–1943	14.21	1797–1807	14.92
1836–1846	14.25	1813–1823	14.80
21 Year			
1978–1998	14.21	1890–1910	14.96
1925–1945	14.32	1946–1966	14.91
1826–1846	14.36	1802–1822	14.78
1866–1886	14.40	1995–2015	14.75

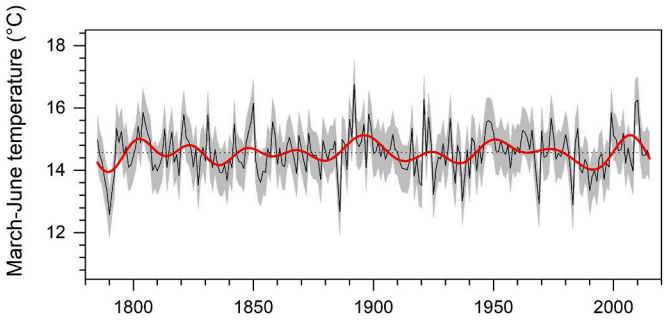

Fig. 3. March–June temperature reconstruction (1785–2015 CE) for the Dokriani glacier region. Red bold line represents the 20 year low pass filter and black dotted line is the long-term mean of the reconstructed series. Shaded area represents the upper and lower error limits.

4.3. Temperature reconstruction

4.3.1. Analyses of March–June temperature reconstruction

The March–June temperature reconstruction resembles well with the instrumental temperature record ($r = 0.65$, $p < 0.00001$, 1898–2015 CE) and captures 42% variance (Fig. 2) (Table 1). Linear trends of the reconstruction and instrumental data further validated the resemblance among both the datasets (Supplementary Fig. S4a). The March–June temperature in both the datasets depicts an increasing trend which is also mirrored by the CRU TS4.06 gridded temperature data (http://climexp.knmi.nl/) for the study area. However, it is less in these months in comparison to that observed in winter and at annual level (Bhutiyani et al., 2007). Borgaonkar et al. (2011) also observed similar variations in the month of March-April-May and June-July-August-September. To understand the variability in sub-periods, we calculated 5, 11, and 21-year running means over the reconstructed series (Table 2). A 5-year running mean showed 1788–1792 CE as the coldest and 1890–1894 CE as the warmest period in the entire record. An 11-year running mean depicted 1986–1996 CE as the coldest and 1890–1900 CE as the warmest followed by 1946–1956 CE and 2000–2010 CE. The 21-year running mean showed 1978–1998 CE, 1925–1945 CE as cool and 1890–1910 CE, 1946–1966 CE as warm periods (Table 2) (Fig. 3). The annual fluctuations in the present reconstruction showed high coherency with those recorded in Feb–June mean temperature reconstruction from Tons region of Uttarakhand ($r = 0.65$, $p < 0.00001$, 1785–2002 CE) (Singh and Yadav, 2014) (Fig. 4a and b). This reconstruction captured cool periods during 1911–1940 CE and warming in 1879–1908 CE and 1941–1970 CE along with the decline in

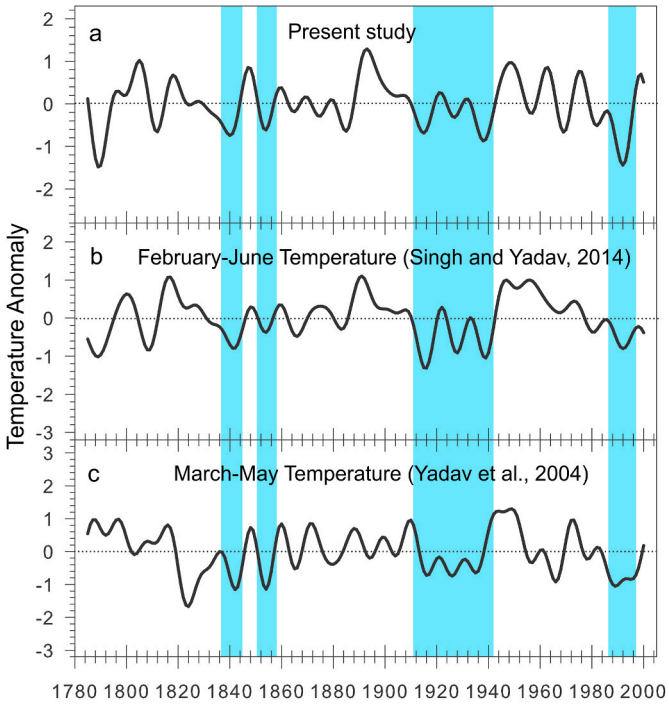

Fig. 4. Comparison of (a) March–June temperature reconstruction with (b) Feb–June temperature reconstruction from Tons valley, Uttarakhand (Singh and Yadav, 2014) and (c) March-April-May temperature reconstruction from Uttarakhand (Yadav et al., 2004). Shaded blue areas represent common cool periods. A 10 year low pass filter was applied to all temperature anomaly series which were derived from mean and standard deviation of temperature data for the common period (1785–2000 CE).

temperature in the last few decades of the 20th century (Fig. 4b) (Singh and Yadav, 2014). Our reconstruction also resembles well ($r = 0.48$, $p < 0.00001$, 1785–2000 CE) with spring (March-April-May) temperature reconstruction showing similar cool and warm phases (Yadav et al., 2004) (Fig. 4c), and with premonsoon (April–May) temperature record from Garhwal Himalaya (Yadav et al., 1997). The temperature variability of the latter half of 20th century captured in these studies from the Western Himalaya were in agreement with our observations of this period with no abnormal warming observed in the reconstruction as well as the instrumental record.

Our record also registers temperature signal at a regional scale. Cool periods in the first half of the 19th century are also observed in temperature records from Karakoram (Esper et al., 2002), and Central Asia (Briffa et al., 2001; Esper et al., 2002) (Table 2). The prominent late 18th century cooling in our record has been captured in Tian Shan (Chen et al., 2019), Tibetan plateau (Xu et al., 2019) and Bhutan (Krusic et al., 2015). And the reconstructions from Nepal (Cook et al., 2003), Tibet and Central Asia (Briffa et al., 2001) are also in agreement with cool phase observed in the last few decades of the 20th century in our reconstruction. Cool phases recorded in 1826–1846 CE, 1910–1920 CE and 1978–1998 CE resembled with the recent temperature reconstruction from southeast Tibet (Yang et al., 2010) (Table 2). Spatial correlation of the March–June reconstructed temperature series with corresponding months gridded data (1901–2015 CE) also endorsed significant association with Western Himalaya, Central Himalaya and the Tibetan plateau, indicating regional scale signatures in our reconstruction (Fig. 5). High spatial correlation ($r \geq 0.5$) was noticed between latitudes ~25°-35°N and longitude ~73°-85°E (Fig. 5).

Low frequency signals captured in our March–June temperature record match with Asia 2k temperature (June-July-August) reconstruction (Pages 2k Consortium, 2013) and northern hemisphere temperature (May-June-July-August) reconstruction (Wilson et al., 2016) (Fig. 6). Cooling in the late 18th century was comparable among the three reconstructions. Low temperature phases during the first half of the 19th century during the Little Ice Age (LIA) in the Asia 2k and Northern hemisphere record was observed as a stable to low phase in our record with, however, a similar fluctuation pattern. A high temperature phase is seen during 1890–1900s CE in Asia 2k and present temperature record, but that is not well registered in the Northern hemisphere record. High temperatures were also recorded in these three records during 1940–1960s CE. Overall, in the 20th century the fluctuation pattern is similar, but steady rise in temperature was observed in the northern hemisphere from the 1910s. However, the Asia 2k record showed this to a lesser degree, whereas March–June temperature showed no such trend (Fig. 6). It is worth noting that these reconstructions correspond to different seasonalities and inclusion/exclusion of months influences the magnitude and is ultimately responsible for variations in trend/-fluctuations among the three reconstructions. The Asia 2k and Northern hemisphere record represent summer months' temperature,

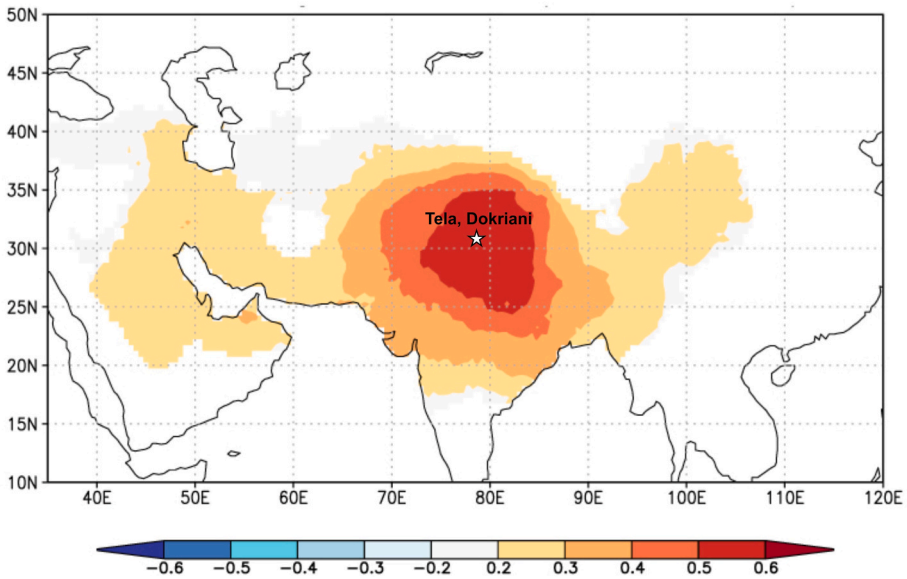

Fig. 5. Spatial correlation between reconstructed March–June temperature and corresponding months' gridded CRU TS4.01 temperature data (1901–2015 CE). Figure was generated using KNMI climate explorer (http://climexp.knmi.nl/).

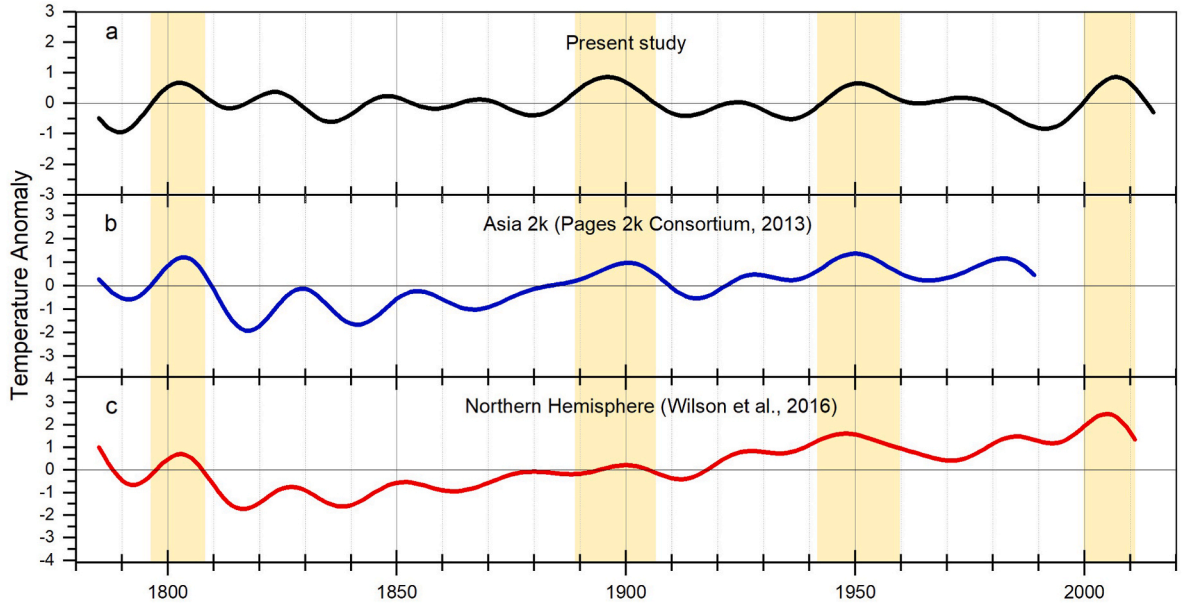

Fig. 6. Comparison of 20 year low pass filtered plots of a) March–June temperature reconstruction (black solid line) with b) Asia 2k June-July-August temperature reconstruction (blue solid line) (Pages 2k Consortium, 2013) and c) Northern hemisphere temperature record (red solid line) (Wilson et al., 2016). Shaded yellow areas represent common warm periods.

June-July-August and May-June-July-August temperature, respectively. Our March–June temperature record has an overlap of only one month (i.e. June) with Asia 2k and two months (i.e. May–June) with Northern hemisphere temperature record and that could be major cause of magnitude difference. Asia 2k record matches well with March–June temperature reconstruction up to 1970 CE. Further, to understand the recent scenario, we analyzed linear trends in sub-periods of recent part (i.e. since 1901 CE up to available data of respective series) of Northern Hemisphere, Asia 2k and the present study (March–June temperature; instrumental and reconstruction), which revealed negligible increase during 1901–1989 CE in March–June temperature record with respect to other two records. However, trends from 1990 CE up to recent available data revealed surge in rise and resembled well with Northern hemisphere record (Supplementary Fig. S4).

To understand in depth the variability and its plausible causes during recent part, we analyzed sub-periods of our March–June temperature record, which showed no significant temperature trend in the 20th century (1901–2000 CE.). However, it captured a slight insignificant increase, supporting the temperature rise, over 1901–2015 CE. This implies that the warming in the 21st century, though not anomalous, has contributed to the rising trend in the region. The March–June instrumental data also depicts an increasing but statistically insignificant trend during entire available period (i.e. 1901-2019 CE). Recent part of reconstruction and instrumental data showed surge in temperature from 1990s, which was also reported by Bhutiyani et al. (2007) in the Western Himalayan region. Low temperature phase observed in our present record during 1980–2000 CE corresponds to decreasing mean temperature because of divergent temperature trends of premonsoon maximum and minimum temperatures, and increase in diurnal temperature range (DTR), in the latter half of the 20th century in the Himalayan region which was associated with large scale land degradation and deforestation (Yadav et al., 2004). Decreasing minimum temperatures (or variability in minimum temperature) trends with respect to maximum temperature has also been recorded by various studies for the north Indian region (Das et al., 2007; Pal and Al-Tabbaa, 2010) as well as the Himalaya (Kumar et al., 1994; Sharma et al., 2000; Arora et al., 2005). The rise in mean temperature in recent decades might be due to decrease in DTR in India (Mall et al., 2021). It has also been observed that cloud cover plays a major role in DTR variability. Low or no cloud cover allows for more radiation to reach the earth's surface causing the daytime maximum temperature to increase, whereas high cloud cover has the opposite effect, thus, decreasing daytime maximum temperature (Pyrgou et al., 2019). Hamal et al. (2021) have reported that high cloud cover causes an increase in overall minimum temperature and decrease in maximum temperature. Therefore, we postulate that recent mean temperature surge could be a result of a rise in minimum temperatures, due to increase in cloud cover associated DTR decrease. However, this needs to be further investigated for better understanding.

To understand the recurrence behavior, we analyzed the spectral characteristics of our March–June temperature reconstruction using the multi-taper method (Mann and Lees, 1996) which revealed peaks at 2.08, 2.61–2.63, 2.67, 2.81–2.89, 3.54–3.55, 3.64–3.68 and 8.83–8.98 year cycles (significant at 99% confidence level) (Supplementary Fig. S5). The shorter periodicities at 2.08, 2.61–2.63, 2.67, 2.81–2.89, 3.54–3.55 and 3.64–3.68 seem to reflect the El Nino Southern Oscillation (ENSO) (Trenberth, 1976) signal of the Pacific Ocean while the periodicities at 8.83–8.98 fall in the range of the Northern Atlantic Oscillation (NAO). A similar ENSO signal was registered in temperature reconstructions in various studies from Western Himalaya (Shah et al., 2019; Singh and Yadav, 2014), Nepal (Thapa et al., 2015; Aryal et al., 2020; Gaire et al., 2020) and Tibetan Plateau (Liang et al., 2008). Peaks within the ENSO variability range were also observed in precipitation records from the Western Himalaya (Singh et al., 2006, 2009; Yadav et al., 2014). Similarly, NAO signal was registered in temperature (Khan et al., 2021) and precipitation (Singh et al., 2009; Yadav, 2011) records from Western Himalaya. The presence of periodicities in our reconstruction within the range of ENSO and NAO cycles suggests that the temperature of our study area is influenced by global circulation systems.

4.3.2. *March–June temperature and Dokriani glacier mass balance linkage*

To understand the relationship between glacier mass balance and temperature, and explore its potential in understanding long-term glacier variability, we correlated the March–June instrumental and reconstructed temperature data with the modelled winter (November–April), summer (May–October) and annual mass balance (Azam and Srivastava, 2020). The analysis revealed high correlation of winter mass balance with instrumental ($r = -0.97$, $p = 0.03$, $n = 4$) and

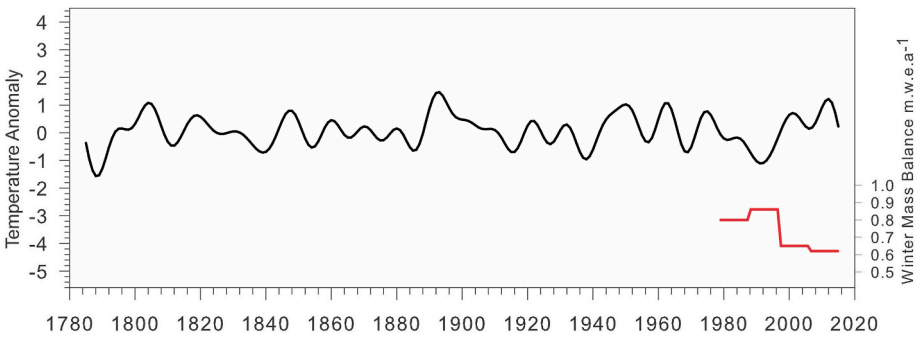

Fig. 7. A 10 year low pass filtered March–June temperature reconstruction (black solid line) plotted with modelled winter mass balance data (1980–2015 CE) (after Azam and Srivastava, 2020). Temperature anomaly series was derived using mean and standard deviation of the 20th century (1901–2000 CE).

reconstructed ($r = -0.98$, $p = 0.02$, $n = 4$) temperature data when average winter mass balance from each of the four periods (1980–1988 CE, 1989–1997 CE, 1998–2006 CE, 2007–2018 CE) used by Azam and Srivastava (2020) to understand the decadal variability was correlated with averaged temperature from the corresponding overlapping periods. On the basis of this significant linkage between winter mass balance and reconstructed temperature we identified periods of mass gain and mass loss, with cool and warm temperature periods registering mass accumulation and ablation, respectively. Thus, cool periods during 1786–1796 CE, 1836–1846 CE, 1910–1920 CE, 1933–1943 CE, and warm periods during, 1890–1900 CE and 1946–1956 CE in our reconstruction could have witnessed mass accumulation and mass wasting episodes, respectively (Fig. 7). Similarly, comparison with the modelled dataset showed that the glacier has witnessed a period of mass gain through the late 1980s CE and 1990s CE, and loss thereafter which increased until 2015 CE (Fig. 7). This trend is mirrored by our temperature reconstruction which depicts cooling during 1986–1996 CE and subsequent temperature high in the 21st century (Azam and Srivastava, 2020). Studies from the Central Himalaya also reveal an increase in temperature and drying in the recent decades (Cannon et al., 2015; Norris et al., 2019). A recent composite annual glacier mass balance reconstruction developed from four glaciers (including Dokriani glacier) in Uttarakhand Himalaya also depicts drastic increase in mass loss in the last 30 years, indicating that the glaciers are in a state of accelerated degradation (Singh et al., 2021). Thus, the phases of mass loss and mass gain identified through comparison between modelled winter mass balance dataset and temperature record are in agreement with other studies in this region, corroborating the strong linkage between temperature and mass balance, and further, indicating its potential in unfolding the Dokriani glacier winter dynamics in the long-term perspective.

5. Conclusions

We developed a ring-width chronology extending back to 1656 CE from Himalayan fir (*A. pindrow*) which was further used to develop March–June temperature reconstruction spanning 231 years (1785–2015 CE) for the Dokriani glacier region, Uttarakhand, Western Himalaya. In the present study, the 21-year running mean periods 1978–1998 CE, 1925–1945 CE, and 1890–1910 CE, 1946–1966 CE were observed as cool and warm, respectively, over the span of the record. The reconstruction captured strong coherence with tree-ring based temperature reconstructions from the Garhwal Himalaya. There was also a broad agreement with other tree-ring based reconstructions from the Western Himalaya, Nepal Himalaya and the Tibetan plateau, indicating the relevance of the reconstruction in understanding climate variability at regional scale. Present record also showed association at low frequency with global temperature record (Asia and Northern Hemisphere). We observed a negligible rise in temperature during 1901–1989 CE with respect to Asia 2k and Northern hemisphere records, however, a surge in rise was observed from 1990 CE that continued in the 21st century, which is also evident in the Northern hemisphere temperature record. We postulate that cloud cover is among the factors governing recent temperature in the region.

March–June temperature reconstruction also showed strong association with Dokriani glacier winter mass balance (November–April), reflecting cool (warm) periods could have witnessed mass accumulation (mass wasting) episodes. Rapid mass loss of the Dokriani glacier since 1990s leading to a rise in mass wasting in the late 20th and early 21st century is in good agreement with rising temperature and increased drying in the Central Himalaya.

Such first temperature record exclusively from the Dokriani region in the upper reaches of the Ganga river, revealing a strong linkage with the Dokriani glacier winter mass balance, provides a valuable dataset in understanding climate variability and glacier response in the past with respect to climate change. This is essential for planning mitigation and resource management strategies in light of the recent and predicted future warming.

Data availability

Data would be available on request.

Funding

This study was funded by the Wadia Institute of Himalayan Geology (An Autonomous Institution of Department of Science & Technology, Government of India), Dehradun, India.

CRediT authorship contribution statement

Tanupriya Rastogi: conceived and designed the study, developed reconstruction, performed analyses, wrote the paper. **Jayendra Singh:** conceived and designed the study, participated in sample collection, generated data, developed reconstruction, performed analyses, wrote the paper. **Nilendu Singh:** participated in sample collection. **Pankaj Chauhan:** participated in sample collection. **Ram R. Yadav:** developed reconstruction, performed analyses, wrote the paper. **Bindhyachal Pandey:** wrote the paper.

Declaration of competing interest

The authors declare that they have no competing interests.

Acknowledgements

Authors (TR, JS, RRY) express their sincere thanks to Director, Wadia Institute of Himalayan Geology, Dehradun for necessary facilities. Generous help offered by the Forest officials of Uttarakhand in collection of research materials is sincerely acknowledged. This work comprises

Wadia Institute of Himalayan Geology contribution number WIHG/0143. Authors express their sincere thanks to the anonymous reviewers for valuable suggestions which substantially improved the manuscript.

Appendix A. Supplementary data

Supplementary data to this article can be found online at https://doi.org/10.1016/j.quaint.2023.05.013.

References

Arora, M., Goel, N.K., Singh, P., 2005. Evaluation of temperature trends over India. Hydrol. Sci. J. 50, 81–93.

Aryal, S., Gaire, N.P., Pokhrel, N.R., Rana, P., Sharma, B., Kharal, D.K., Poudel, B.S., Dyola, N., Fan, Z.-X., Grießinger, J., Bräuning, A., 2020. Spring season in western Nepal Himalaya is not yet warming: a 400-year temperature reconstruction based on tree-ring widths of Himalayan Hemlock (Tsuga dumosa). Atmosphere 11, 132.

Azam, M.F., Srivastava, S., 2020. Mass balance and runoff modelling of partially debris-covered Dokriani Glacier in monsoon-dominated Himalaya using ERA5 data since 1979. J. Hydrol. 590, 125432.

Bhattacharyya, A., Chaudhary, V., 2003. Late-summer temperature reconstruction of the eastern Himalayan region based on tree-ring data of Abies densa. Arctic Antarct. Alpine Res. 35, 196–202.

Bhattacharyya, A., Ranhotra, P.S., Gergan, J.T., 2011. Vegetation vis-a-vis climate and glacier history during 12,400 to 5,400 yr BP from Dokriani valley, Garhwal Himalaya, India. J. Geol. Soc. India 77 (5), 401–408.

Bhutiyani, M.R., Kale, V.S., Pawar, N.J., 2007. Long-term trends in maximum, minimum and mean annual air temperatures across the Northwestern Himalaya during the twentieth century. Clim. Change 85, 159–177.

Biondi, F., Waikul, K., 2004. DENDROCLIM2002: a C++ program for statistical calibration of climate signals in tree-ring chronologies. Comput. Geosci. 30, 303–311.

Borgaonkar, H.P., Pant, G.B., Rupa Kumar, K., 1996. Ring-width variations in Cedrus deodara and its climatic response over the western Himalaya. Int. J. Climatol. 16, 1409–1422.

Borgaonkar, H.P., Pant, G.B., Kumar, K.R., 1999. Tree-ring chronologies from western Himalaya and their dendroclimatic potential. IAWA J. 20, 295–309.

Borgaonkar, H.P., Sikder, A.B., Ram, S., 2011. High altitude forest sensitivity to the recent warming: a tree-ring analysis of conifers from Western Himalaya, India. Quat. Int. 236 (1–2), 158–166.

Briffa, K.R., Osborn, T.J., Schweingruber, F.H., Harris, I.C., Jones, P.D., Shiyatov, S.G., Vaganov, E.A., 2001. Low-frequency temperature variations from a northern tree ring density network. J. Geophys. Res. Atmos. 106, 2929–2941.

Cannon, F., Carvalho, L.M., Jones, C., Bookhagen, B., 2015. Multi-annual variations in winter westerly disturbance activity affecting the Himalaya. Clim. Dynam. 44, 441–455.

Champion, H.G., Seth, S.K., 1968. A Revised Survey of the Forest Types of India. Manager of Publication, Government of India, New Delhi.

Chaudhary, V., Bhattacharyya, A., Guiot, J., Shah, S.K., Srivastava, S.K., Edouard, J.L., Thomas, A., 2013. Reconstruction of August-September Temperature in North-Western Himalaya since AD 1773, Based on Tree-Ring Data of Pinus Wallichiana and Abies Pindrow. Holocene: Perspectives, Environmental Dynamics and Impact Events; Nova Science Publishers, New York, NY, USA, pp. 145–156.

Chen, F., Yuan, Y., Yu, S., Chen, F., 2019. A 391-year summer temperature reconstruction of the Tien Shan, reveals far-reaching summer temperature signals over the midlatitude Eurasian continent. J. Geophys. Res. Atmos. 124 (22), 11850–11862.

Cook, E.R., Briffa, K.R., Shiyatov, S., Mazepa, V., 1990. Tree-ring standardization and growth-trend estimation. In: Methods of Dendrochronology: Applications in the Environmental Sciences, pp. 104–123.

Cook, E.R., Meko, D.M., Stahle, D.W., Cleaveland, M.K., 1999. Drought reconstructions for the continental United States. J. Clim. 12, 1145–1162.

Cook, E.R., Krusic, P.J., Jones, P.D., 2003. Dendroclimatic signals in long tree-ring chronologies from the Himalayas of Nepal. Int. J. Climatol. 23, 707–732.

Dai, A., 2013. Increasing drought under global warming in observations and models. Nat. Clim. Change 3, 52–58. https://doi.org/10.1038/nclimate1633.

Das, S.K., Jenamani, R.K., Kalsi, S.R., Panda, S.K., 2007. Some evidence of climate change in twentieth-century India. Clim. Change 85, 299–321. https://doi.org/10.1007/s10584-007-9305-9.

Diaz, H.F., Bradley, R.S., 1997. Temperature variations during the last century at high elevation sites. In: Climatic Change at High Elevation Sites. Springer, Dordrecht, pp. 21–47.

Dobhal, D.P., Gergan, J.T., Thayyen, R.J., 2004. Recession and morphogeometrical changes of Dokriani glacier (1962-1995) Garhwal Himalaya, India. Curr. Sci. 86, 692–696.

Dobhal, D.P., Gergan, J.T., Thayyen, R.J., 2008. Mass balance studies of the Dokriani glacier from to, Garhwal Himalaya, India. Bull. Glaciol. Res. 25, 9–17.

Dobhal, D.P., Mehta, M., 2010. Surface morphology, elevation changes and terminus retreat of Dokriani Glacier, Garhwal Himalaya: implication for climate change. Himal. Geol. 31, 71–78.

Donat, M., Lowry, A., Alexander, L., et al., 2016. More extreme precipitation in the world's dry and wet regions. Nat. Clim. Change 6, 508–513. https://doi.org/10.1038/nclimate2941.

Duchenne-Moutien, R.A., Neetoo, H., 2021. Climate change and emerging food safety issues: a review. J. Food Protect. 84 (11), 1884–1897.

Esper, J., Schweingruber, F.H., Winiger, M., 2002. 1300 years of climatic history for Western Central Asia inferred from tree-rings. Holocene 12, 267–277.

Fischer, E., Knutti, R., 2015. Anthropogenic contribution to global occurrence of heavy-precipitation and high-temperature extremes. Nat. Clim. Change 5, 560–564. https://doi.org/10.1038/nclimate2617.

Fritts, H.C., 1976. Tree-Rings and Climate. Academic Press, San Diego, California.

Gaire, N.P., Fan, Z.X., Bräuning, A., Panthi, S., Rana, P., Shrestha, A., Bhuju, D.R., 2020. Abies spectabilis shows stable growth relations to temperature, but changing response to moisture conditions along an elevation gradient in the central Himalaya. Dendrochronologia 60, 125675.

Garg, P.K., Yadav, J.S., Rai, S.K., Shukla, A., 2022. Mass balance and morphological evolution of the Dokriani Glacier, central Himalaya, India during 1999–2014. Geosci. Front. Times 13 (1), 101290.

Hamal, K., Sharma, S., Talchabhadel, R., Ali, M., Dhital, Y.P., Xu, T., Dawadi, B., 2021. Trends in the diurnal temperature range over the southern slope of central Himalaya: retrospective and prospective evaluation. Atmosphere 12 (12), 1683.

Hasnain, S.I., Thayyen, R.J., 1999. Discharge and suspended-sediment concentration of meltwaters, draining from the Dokriani glacier, Garhwal Himalaya, India. J. Hydrol. 218, 191–198.

Hasnain, S.I., Jose, P.G., Ahmad, S., Negi, D.C., 2001. Character of the subglacial drainage system in the ablation area of Dokriani glacier, India, as revealed by dye-tracer studies. J. Hydrol. 248, 216–223.

Heim, A., Gansser, A., 1939. Central Himalaya. Hindustan Publishing, Delhi.

Holmes, R.L., 1983. Computer-assisted quality control in tree-ring dating and measurement. Tree-Ring Bull. 43, 69–78.

Horton, R.M., Mankin, J.S., Lesk, C., Coffel, E., Raymond, C., 2016. A review of recent advances in research on extreme heat events. Curr. Clim. Change Rep. 2 (4), 242–259.

IPCC, 2021. Summary for policymakers. In: Zhai, P., Pirani, A., Connors, S.L., Péan, C., Berger, S., Caud, N., Chen, Y., Goldfarb, L., Gomis, M.I., Huang, M., Leitzell, K., Lonnoy, E., Matthews, J.B.R., Maycock, T.K., Waterfield, T., Yelekçi, O., Yu, R., Zhou, B. (Eds.), Climate Change 2021: the Physical Science Basis. Contribution of Working Group I to the Sixth Assessment Report of the Intergovernmental Panel on Climate Change [Masson-Delmotte, V. Cambridge University Press (in press).

Kattel, D.B., Yao, T., Yang, K., Tian, L., Yang, G., Joswiak, D., 2013. Temperature lapse rate in complex mountain terrain on the southern slope of the central Himalayas. Theor. Appl. Climatol. 113 (3), 671–682.

Khan, A., Ahmed, M., Gaire, N.P., Iqbal, J., Siddiqui, M.F., Khan, A., et al., 2021. Tree-ring-based temperature reconstruction from the western Himalayan region in northern Pakistan since 1705 CE. Arabian J. Geosci. 14, 1–12.

Kraaijenbrink, P.D.A., Bierkens, M.F.P., Lutz, A.F., Immerzeel, W.W., 2017. Impact of a global temperature rise of 1.5 degrees Celsius on Asia's glaciers. Nature 549, 257–260.

Krusic, P.J., Cook, E.R., Dukpa, D., Putnam, A.E., Rupper, S., Schaefer, J., 2015. Six hundred thirty-eight years of summer temperature variability over the Bhutanese Himalaya. Geophys. Res. Lett. 42, 2988–2994.

Kumar, K.R., Kumar, K.K., Pant, G.B., 1994. Diurnal asymmetry of surface temperature trends over India. Geophys. Res. Lett. 21 (8), 677–680.

Kumar, A., Verma, A., Dobhal, D.P., Mehta, M., Kesarwani, K., 2014. Climatic control on extreme sediment transfer from Dokriani Glacier during monsoon, Garhwal Himalaya (India). J. Earth Syst. Sci. 123, 109–120.

Levy, B., Patz, J., 2015. Climate Change and Public Health. Oxford University Press.

Liang, E., Shao, X., Qin, N., 2008. Tree-ring based summer temperature reconstruction for the source region of the Yangtze River on the Tibetan Plateau. Global Planet. Change 61, 313–320.

Malik, R., Rossi, S., Sukumar, R., 2020. Variations in the timing of different phenological stages of cambial activity in Abies pindrow (Royle) along an elevation gradient in the north-western Himalaya. Dendrochronologia 59, 125660.

Mall, R.K., Chaturvedi, M., Singh, N., Bhatla, R., Singh, R.S., Gupta, A., Niyogi, D., 2021. Evidence of asymmetric change in diurnal temperature range in recent decades over different agro-climatic zones of India. Int. J. Climatol. 41 (4), 2597–2610.

Mann, M.E., Lees, J.M., 1996. Robust estimation of background noise and signal detection in climatic time series. Clim. Change 33, 409–445.

Meehl, G.A., Tebaldi, C., 2004. More intense, more frequent, and longer lasting heat waves in the 21st century. Science 305, 994–997.

Mondal, A., Khare, D., Kundu, S., 2015. Spatial and temporal analysis of rainfall and temperature trend of India. Theor. Appl. Climatol. 122 (1), 143–158.

Negi, S.S., 2000. Himalayan Forests and Forestry. Indus Publishing.

Neukom, R., Gergis, J., Karoly, D., et al., 2014. Inter-hemispheric temperature variability over the past millennium. Nat. Clim. Change 4, 362–367. https://doi.org/10.1038/nclimate2174.

Norris, J., Carvalho, L.M.V., Jones, C., Cannon, F., 2019. Deciphering the contrasting climatic trends between the central Himalaya and Karakoram with 36 years of WRF simulations. Clim. Dynam. 52, 159–180.

Ohmura, A., 2012. Enhanced temperature variability in high-altitude climate change. Theor. Appl. Climatol. 110 (4), 499–508.

Pages 2k Consortium, 2013. Continental-scale temperature variability during the past two millennia. Nat. Geosci. 6, 339–346.

Pal, I., Al-Tabbaa, A., 2010. Long-term changes and variability of monthly extreme temperatures in India. Theor. Appl. Climatol. 100, 45–46. https://doi.org/10.1007/s00704-009-0167.

Pepin, N., Bradley, R.S., Diaz, H.F., Baraer, M., Caceres, E.B., Forsythe, N., Fowler, H., Greenwood, G., Hashmi, M.Z., Liu, X.D., Miller, J.R., Ning, L., Ohmura, A., Palazzi, E., Rangwala, I., Schöner, W., Severskiy, I., Shahgedanova, M., Wang, M.B.,

Williamson, S.N., Yang, D.Q., 2015. Elevation-dependent warming in mountain regions of the world. Nat. Clim. Change. https://doi.org/10.1038/NCLIMATE2563.
Phadtare, N.R., 2000. Sharp decrease in summer monsoon strength 4000–3500 cal yr BP in the Central Higher Himalaya of India based on pollen evidence from alpine peat. Quat. Res. 53 (1), 122–129.
Pratap, B., Dobhal, D.P., Mehta, M., Bhambri, R., 2015. Influence of debris cover and altitude on glacier surface melting: a case study on Dokriani Glacier, central Himalaya, India. Ann. Glaciol. 56, 9–16.
Pratap, B., Dobhal, D.P., Bhambri, R., Mehta, M., Tewari, V.C., 2016. Four decades of glacier mass balance observations in the Indian Himalaya. Reg. Environ. Change 16, 643–658.
Pyrgou, A., Santamouris, M., Livada, I., 2019. Spatiotemporal analysis of diurnal temperature range: effect of urbanization, cloud cover, solar radiation, and precipitation. Climate 7 (7), 89.
Ram, S., 2012. Tree growth–climate relationships of conifer trees and reconstruction of summer season Palmer Drought Severity Index (PDSI) at Pahalgam in Srinagar, India. Quat. Int. 254, 152–158.
Rinn, F., 2003. TSAPWin: Time Series Analysis and Presentation for Dendrochronology and Related Applications– Frank Rinn (Heidelberg, Germany).
Sano, M., Furuta, F., Kobayashi, O., Sweda, T., 2005. Temperature variations since the mid-18th century for western Nepal, as reconstructed from tree-ring width and density of Abies spectabilis. Dendrochronologia 23, 83–92.
Shah, N.C., Joshi, M.C., 1971. An ethnobotanical study of the Kumaon region of India. Econ. Bot. 25 (4), 414–422. http://www.jstor.org/stable/4253291.
Shah, S.K., Pandey, U., Mehrotra, N., Wiles, G.C., Chandra, R., 2019. A winter temperature reconstruction for the Lidder Valley, Kashmir, Northwest Himalaya based on tree-rings of Pinus wallichiana. Clim. Dynam. 53, 4059–4075.
Sharma, K.P., Moore, B., Vorosmarty, C.J., 2000. Anthropogenic, climatic, and hydrologic trends in the Kosi basin, Himalaya. Clim. Change 47 (1), 141–165.
Shrestha, A.B., Wake, C., Mayewski, P., Dibb, J., 1999. Maximum temperature trends in the Himalaya and vicinity: an analysis based on temperature records from Nepal for the period 1971–94. J. Clim. 12, 2775–2786.
Singh, J., Yadav, R.R., 2005. Spring precipitation variations over the western Himalaya, India, since AD 1731 as deduced from tree rings. J. Geophys. Res. Atmos. 110 (D1).
Singh, J., Park, W.K., Yadav, R.R., 2006. Tree-ring-based hydrological records for western Himalaya, India, since AD 1560. Clim. Dynam. 26, 295–303.
Singh, J., Yadav, R.R., Wilmking, M., 2009. A 694-year tree-ring based rainfall reconstruction from Himachal Pradesh, India. Clim. Dynam. 33, 1149.
Singh, J., Yadav, R.R., 2014. February–June temperature variability in western Himalaya, India, since AD 1455. Quat. Int. 349, 98–104.
Singh, J., Singh, N., Chauhan, P., Yadav, R.R., Bräuning, A., Mayr, C., Rastogi, T., 2019. Tree-ring δ18O records of abating June–July monsoon rainfall over the Himalayan region in the last 273 years. Quat. Int. 532, 48–56.
Singh, N., Shekhar, M., Singh, J., Gupta, A.K., Bräuning, A., Mayr, C., Singhal, M., 2021. Central Himalayan tree-ring isotopes reveal increasing regional heterogeneity and enhancement in ice mass loss since the 1960s. Cryosphere 15, 95–112.
Singh, P., Haritashya, U.K., Kumar, N., 2004. Seasonal changes in meltwater storage and drainage characteristics of the Dokriani Glacier, Garhwal Himalayas (India). Nord. Hydrol 35, 15–29.
Sonali, P., Kumar, D.N., Nanjundiah, R.S., 2017. Intercomparison of CMIP5 and CMIP3 simulations of the 20th century maximum and minimum temperatures over India and detection of climatic trends. Theor. Appl. Climatol. 128 (1–2), 465–489.
Stokes, M.A., Smiley, T.L., 1968. An Introduction to Tree-Ring Dating (Reprinted 1996). Univ. of Ariz. Press, Tucson.
Teskey, R., Wertin, T., Bauweraerts, I., Ameye, M., McGuire, M.A., Steppe, K., 2015. Responses of tree species to heat waves and extreme heat events. Plant Cell Environ. 38 (9), 1699–1712.
Thapa, U.K., Shah, S.K., Gaire, N.P., Bhuju, D.R., Bhattacharyya, A., Thagunna, G.S., 2013. Influence of climate on radial growth of Abies pindrow in Western Nepal Himalaya. Banko Janakari 23, 14–19.
Thapa, U.K., Shah, S.K., Gaire, N.P., Bhuju, D.R., 2015. Spring temperatures in the far-western Nepal Himalaya since AD 1640 reconstructed from Picea smithiana tree-ring widths. Clim. Dynam. 45, 2069–2081.
Thayyen, R.J., Gergan, J.T., Dobhal, D.P., 2005. Monsoonal control on glacier discharge and hydrograph characteristics, a case study of Dokriani Glacier, Garhwal Himalaya, India. J. Hydrol. 306, 37–49.
Thayyen, R.J., Gergan, J.T., Dobhal, D.P., 2007. Role of glaciers and snow cover on headwater river hydrology in monsoon regime—micro-scale study of Din Gad catchment, Garhwal Himalaya, India. Curr. Sci. 376–382.
Thayyen, R.J., Gergan, J.T., 2010. Role of glaciers in watershed hydrology: a preliminary study of a " Himalayan catchment". Cryosphere 4, 115–128.
Trenberth, K.E., 1976. Spatial and temporal variations of the southern oscillation. Q. J. R. Meteorol. Soc. 102, 639–653.
Valdiya, K.S., 1998. Dynamic Himalaya. Universities Press.
Wigley, T.M.L., Briffa, K.R., Jones, P.D., 1984. On the average value of correlated time series with applications in dendroclimatology and hydrometeorology. J. Clim. Appl. Meteorol. 23, 201–213.
Wilson, R., Anchukaitis, K., Briffa, K.R., Büntgen, U., Cook, E., D'Arrigo, R., Davi, N., Esper, J., Frank, D., Gunnarson, B., Hegerl, G., Helama, S., Klesse, S., Krusic, P.J., Linderholm, H.W., Myglan, V., Osborn, T.J., Rydval, M., Schneider, L., Schurer, A., Wiles, G., Zhang, P., Zorita, E., 2016. Last millennium northern hemisphere summer temperatures from tree rings: Part I: the long term context. Quat. Sci. Rev. 134, 1–18.
Worm, B., Lotze, H.K., 2021. Marine biodiversity and climate change. In: Climate Change. Elsevier, pp. 445–464.
Xu, J., Grumbine, R., Shrestha, A., Eriksson, M., Yang, X., Wang, Y., Wilkes, A., 2009. The melting Himalayas: cascading effects of climate change on water, biodiversity, and livelihoods. Conserv. Biol. 23, 520–530.
Xu, G., Liu, X., Zhang, Q., Zhang, Q., Hudson, A., Trouet, V., 2019. Century-scale temperature variability and onset of industrial-era warming in the Eastern Tibetan Plateau. Clim. Dynam. 53 (7), 4569–4590.
Yadav, R.R., 2011. Long-term hydroclimatic variability in monsoon shadow zone of western Himalaya, India. Clim. Dynam. 36, 1453–1462.
Yadav, R.R., Park, W.K., Bhattacharyya, A., 1997. Dendroclimatic reconstruction of April–May temperature fluctuations in the western Himalaya of India since AD 1698. Quat. Res. 48, 187–191.
Yadav, R.R., Park, W.K., Bhattacharyya, A., 1999. Spring-temperature variations in western Himalaya, India, as reconstructed from tree-rings: AD 1390-1987. Holocene 9, 85–90.
Yadav, R.R., Park, W.K., 2000. Precipitation reconstruction using ring-width chronology of Himalayan cedar from western Himalaya: preliminary results. J. Earth Syst. Sci. 109 (3), 339–345.
Yadav, R.R., Park, W.K., Singh, J., Dubey, B., 2004. Do the western Himalayas defy global warming? Geophys. Res. Lett. 31 (17).
Yadav, R.R., Misra, K.G., Kotlia, B.S., Upreti, N., 2014. Premonsoon precipitation variability in Kumaon Himalaya, India over a perspective of~ 300 years. Quat. Int. 325, 213–219.
Yang, B., Kang, X., Bräuning, A., Liu, J., Qin, C., Liu, J., 2010. A 622-year regional temperature history of southeast Tibet derived from tree rings. Holocene 20, 181–190.
Zhu, H.F., Shao, X.M., Yin, Z.Y., Huang, L., 2011. Early summer temperature reconstruction in the eastern Tibetan Plateau since AD 1440 using tree-ring width of Sabina tibetica. Theor. Appl. Climatol. 106, 45–53.